A Robust Fixed-Time Torch Height Control based on Finite-Time Observer to compensate the Plasma Jet's Power Fluctuation under Compressed Gas O_2 Plasma/Air shield as the CNC Plasma Machine's Uncertainties in Mild Steel Cutting Process

Varin Cholahan and Tassaphan Suwannatat*

EEC Networking of Mechatronics Excellent Center, School of Engineering and Innovation,
Rajamangala University of Technology Tawan-ok
E-mail: varin.chol@gmail.com, tassaphan.su@rmutto.ac.th*

Abstract

This research started from the collaboration between the Federation of Pathum Thani Industries, Delta Electronics (Thailand) Public Company Limited, and the Department of Mechatronics and Robotics Engineering, Rajamangala University of Technology Tawan-ok. The industrial entrepreneur who is a member of the Federation of Pathum Thani Industries came to consult about the CNC Plasma machine, Hypertherm HPR260 with power 26,000W, purchased at a price of 8,000,000 baht, but it has been damaged and unusable for 5 years. Most of the damage is the electrical control system, but the mechanical structure is still in good condition. The entrepreneur realized that the machine should be able to be retrofitted and be usable again without having to buy a new machine. The Department of Mechatronics and Robotics Engineering has carried out the retrofitting of the CNC Plasma machine to make it usable. The fund was supported by machine owner. After retrofitting, it was later found that there exits some technical issue, when encountering a long metal sheet or a metal sheet with unequal levels. These issues cause the cutting surface of workpiece uneven. Some workpiece had convex cutting surface, while some had concave surfaces. The study found that setting the Z-axis lift distance constant while the X and Y axes moved made the Square region of the plasma gas profile in contact with the metal not constant. In order to keep the range of Square cut region constant during metal cutting process, the research team started to develop a Torch Height Control (THC) system by first solving the issue with a PID Controller and later developed it into a Fixed-Time Controller. In this research, Fixed-Time controller along with the Finite-Time Exact Observer (FTSMC-FEO) is a step further development to vanish Plasma Arc Machines' uncertainties.

Keywords: Practical Fixed-Time Control, Nonlinear control, Torch Height Control (THC), Finite Exact Observer (FEO), Plasma Arc Machines (PAM).

1. Introduction

The plasma arc cutting process uses a transferred electric arc established between the negative electrode within a plasma cutting torch and the workpiece. The plasma jet generated by the transferred arc needs to be narrow and have sufficient power density so that the heat diffusion across the thickness of the metallic plate is fast to obtain a narrow kerf of cut. Further, the momentum of the plasma jet should be high so that the force exerted by the jet on the molten is high enough to displace the material from the zone of cut rapidly without adhering to the bottom of the plate to form what is known as dross.

Plasma Arc Machines (PAM) can cut high-strength materials accurately and quickly using gases such as O_2, N_2 or Ar [1]. PAM can provide faster production at a lower cost compared to other cutting processes. The PAM utilizes a plasma gas to cut the material. High-pressure plasma melt and eliminate material from the workpiece. High electrical current is used to produce a plasma jet between the electrode and workpiece with temperature about 20,000 degrees Celsius. Therefore, the characteristics of the plasma arc are complicated. Traditional linear control strategies are difficult to face the uncertainties of plasma cutting [2]. Plasm Arc Process is a nonlinear process. It occupied by complicated uncertainties. To relieve this difficult, the nonlinearities and external disturbances are estimated and compensated by and the Finite-Time Exact Observer (FEO) and thus the need of the complex uncertainties information is effectively avoided [3], [4]. The Torch Height Control (THC) of CNC Plasma Arc Machines (PAM) is directly relating to cutting quality. To regulate the Square cut region constant, a novel Robust Fixed-Time Sliding Mode Control (FTSMC) is introduced to maintain Torch-to-Work distance invariably This method automatically adjusts the Z Lifting Axis position to hold the specified target Arc Voltage for the best possible cuts [5].

To develop research to the next level, this paper presents a novel algorithm to enhance the dynamic performance of cutting quality with more robustness by using FEO. It is a further development from my latest research. Firstly, a novel sliding surface is chosen. Secondly, to cope with uncertainties, Finite-Time Exact Observer (FEO) has been formulated. Then, a practical fixed-time algorithm is proposed and stability analysis method of Lyapunov function is presented to demonstrate the system stability. Eventually, the numerical simulations are illustrated to verify our control scheme. The experimentation with HPR260 Hypertherm Plasma module is set up. Delta CNC Controller with high precision servo motors and drives are employed.

*Corresponding Author

2. Preliminaries

2.1 Plasma Arc Machines' Torch

Torch Height Control (THC) consists of motion controller and sensor device. THC sensor measures arc voltage. Higher gab between the plasma torch and metal results in higher the voltage. So based on the measured voltage value we can manipulate a height of plasma torch to yield an unfluctuating Arc voltage. Torch Height Controller then sends control signals to compensates Torch movement. Fig. 1. is Arc profile from Plasma Arc Machine's Torch. In this research, compressed gas O_2 is ignited as Plasma. Air is utilized as shield.

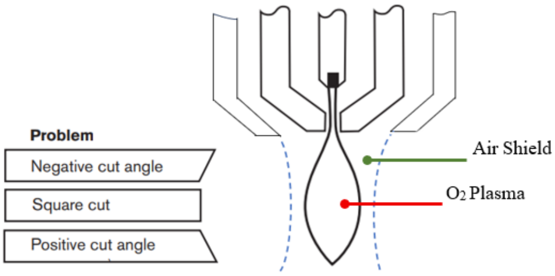

Fig. 1 Arc Profile from Plasma Arc Machines.

To have a cutting quality, controller needs to maintain the range of Square region to machine the steel plate under unpredictable sources of uncertainties and disturbances.

2.2 Fixed-Time Control

General form of second order dynamic system can be represented by

$$\begin{aligned} \dot{x}_1 &= x_2 \\ \dot{x}_2 &= g(x)u + N(x) + d(x,t) \end{aligned} \tag{1}$$

where x is the state vector; $N(x)$ and $g(x)$ are continuous differentiable function and bounded by positive real number. Bounded disturbance and bounded input represent by $d(x,t)$ and u respectively.

Definition (i) The dynamic system (1) is a global finite-time stable if and only if it is Lyapunov stable, and for all $x_0 \in R^n$ there exists $T(x_0) \geq 0$ depending on the initial condition such that, for any $x(\cdot)$ solution of (1) with $x(0) = x_0, \lim_{t \to T(x_0)} \|x(t)\| = 0$, i.e., for all $t \geq T(x_0)$. The function T is called settling time.

Definition (ii) System (1) is global fixed-time stable if: *(I)* The system is globally finite-time stable. *(II)* Function T is upper bound where $T > 0$, for all $x_0 \in R^n$, $T(x_0) \leq T$, and T is not dependent on initial values.

Definition (iii) For any $\alpha > 0$, $x \in R$, a nonlinear function is defined as: $sign^{\alpha}(x) = sign(x)|x|^{\alpha}$, $sign(x) = \{+1 \; or -1\}$.

Lemma 1: If there is a differentiable positive definite radially unbounded function $V : R^n \to R^+$ such that

$$\dot{V}(x) \leq -\alpha_1 V(x)^{\kappa} - \alpha_2 V(x)^{\varphi} + \nu \tag{2}$$

where $x \in R^n, a_1 > 0, a_2 > 0, \nu > 0$, and $0 < \kappa < 1 < \varphi$, then the system (1) is practical fixed-time stable. The reaching time is $T \leq \frac{1}{\alpha_1 \varsigma (1-\kappa)} + \frac{1}{\alpha_2 \varsigma (\varphi - 1)}$ with $0 < \varsigma < 1$. The trajectory converges into the neighborhood residual sets described by $\Phi \in \left\{ V(x) \leq (\frac{\nu}{(1-\varsigma)\alpha_1})^{1/\kappa}, (\frac{\nu}{(1-\varsigma)\alpha_2})^{1/\varphi} \right\}$.

Remark 1: the meaning of "practical" in Lemma 1 is a general idea that the tracking error does not approach to the zero ideally, but to a residual set of the neighborhoods of origin as in most application cases.

Lemma 2 [6]: Define the dynamical system as

$$\dot{x} = -\frac{1}{\Xi(x)} \left(\beta_1 sign(x)^{1+\gamma_1} + \eta_1 sign(x)^{\frac{n_1}{m_1}} \right) \tag{3}$$

where $sign(x)$ is complied with *Definition (iii)*; $\Xi(x)$ is a time-varying gain function and is denoted as $\Xi(x) = a_1 + (1 - a_1)\exp(-b_1 |x|^{c_1})$, $\gamma_1 = \frac{q_1}{p_1}(1 + sign(|x| - 1))$; $\beta_1 > 0, \eta_1 > 0, 0 < a_1 < 1$ and $b_1 > 0$; c_1 is a positive even integer; m_1, n_1, p_1 and q_1 are positive odd integers with $n_1 < m_1$, $p_1 < q_1$.

By Lemma 1, the dynamic system (3) is fixed-time stable system and its reaching time is shown below:

Proof: Letting $y = |x|^{\frac{m_1 - n_1}{m_1}}$ and combining (3), lead to the equation

$$\begin{aligned} \dot{y} &= \frac{m_1 - n_1}{m_1 \Xi(x) sign(x)^{n_1/m_1}} \left(\beta_1 sign(x)^{1+\gamma_1} + \eta_1 sign(x)^{\frac{n_1}{m_1}} \right) \\ &= \frac{m_1 - n_1}{m_1 \Xi(x)} \left(\beta_1 y^{1+\gamma_1 \frac{m_1 - n_1}{m_1}} + \eta_1 \right) \end{aligned}.$$

By computing above equation, the convergence time is obtained by

$$T_a \leq \frac{m_1}{m_1 - n_1} \left(\int_0^1 \frac{\Xi(x)}{\beta_1 y + \eta_1} dy + \int_0^{y_0} \frac{\Xi(x)}{\beta_1 y^{\varepsilon_1} + \eta_1} dy \right)$$

where $\varepsilon_1 = 1 + \frac{m_1 q_1}{p_1 (m_1 - n_1)}$. Because of $a_1 \leq \Xi(x) \leq 1$, the supremum of T_a is given by

$$T_a \leq \frac{m_1}{m_1 - n_1} \left(\int_0^1 \frac{1}{\beta_1 y + \eta_1} dy + \int_0^{y_0} \frac{1}{\beta_1 y^{\varepsilon_1}} dy \right)$$

and resulting to

$$T_a \leq \frac{m_1}{\beta_1 (m_1 - n_1)} \ln \left(\frac{\beta_1 + \eta_1}{\eta_1} \right) + \frac{p_1}{\beta_1 q_1}. \tag{4}$$

It is emphasized that T_a is not related to the initial condition.

2.3 Plasma Torch Mathematical Model

The free body diagram of Plasma Machine's Torch is shown in Fig. 2. Torch is moved and subjected to uncertainties, load disturbances and forces exerted on its body. It is equivalent to the nonlinear mass-spring system.

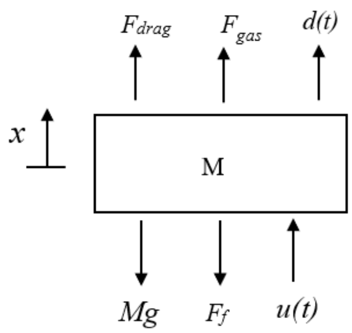

Fig. 2 Free body diagram of Plasma Machine's Torch under uncertainties and external disturbances.

Drag force is caused by air shield with high pressure and high speed mass flow rate demonstrated by

$$F_{drag} = \frac{1}{2}\rho A C_d \upsilon^2 \tag{5}$$

where the parameters ρ, A, and C_d refer to the air density, against frontal area, and drag coefficient, respectively.

The axial force of jet is obtained by integrating radially the momentum of the plasma jet as given by

$$F_{gas} = \int_0^{r_n} \rho c^2 2\pi r\, dr \tag{6}$$

where ρ is the mass density of plasma, c is the sonic velocity, and h is enthalpy. The radial coordinate is r, which varies from the axis of the arc to the nozzle radius r_n. Parameters in (5) and (6) are actually time varying, hard predictable and multivariable-coupled. It is quite difficult to have a complete model. To overcome the difficulty of modeling, these variables will be grouped as a lumped perturbation and the observer is efficiently used for estimating these lump uncertainties.

The nonlinear mathematical model can be considered as

$$M\ddot{x}(t) + kx(t) + F_f + F_{gas} + F_{drag} = u(t) \tag{7}$$

In the above expressions, $x(t)$, $u(t)$, k, g, M, μ and sgn(.) is the mass position, the system input, spring coefficient, gravity constant, mass value, friction coefficient and the signum function respectively. Under the uncertainties and disturbances, the nonlinear mass-spring system (7) in the state-space can be written as

$$\begin{aligned} \dot{x}_1 &= x_2 \\ \dot{x}_2 &= g(x)u + N_0(x) + \Delta f(x) + d(x,t) \end{aligned} \tag{8}$$

where $N_0(x) = -\frac{1}{M}\left(k_0 x_1 + \mu_0 g\, \mathrm{sgn}(x_2) + F_{gas,0} + F_{drag,0}\right)$, x are state matrix, the nonlinear variation function $\Delta f(x)$ and $d(x,t)$ external disturbances respectively. With small distance of movement, Mg can be neglected.

2.4 Controller and Observer Design

Tracking error can be defined as:

$$e = x - x_r \ . \tag{9}$$

Thus, by setting $x_1 = e$, $x_2 = \dot{e} = \dot{x} - \dot{x}_r$, the close-loop error dynamics of Torch's position can be written as

$$\begin{aligned} \dot{x}_1 &= x_2 \\ \dot{x}_2 &= \frac{1}{M}U + N_0(x) + \sigma(t) - \ddot{x}_r \end{aligned} \tag{10}$$

where $\sigma(t) = \dfrac{\Delta f(x) + d(x,t)}{M}$.

Note that for the lumped term $\sigma(t)$ and its derivative are bounded by positive constants.

Proposition 1: The control signal proposed as:

$$U_{in} = M(U_{eq} + U_b - N_0(x) - \hat{\sigma}) \tag{11a}$$

$$\begin{aligned} U_{eq} &= \ddot{x}_r \\ &- \frac{1}{\Xi(e)}\left(\beta_1(1+\gamma_1)diag(|e|)^{\gamma_1} + \frac{\eta_1 n_1}{m_1} diag(e)^{\frac{n_1}{m_1}}\right) \\ &+ \frac{\dot{\Xi}(e)}{\Xi^2(e)}\left(\beta_1 sign(e)^{1+\gamma_1} + \eta_1 sign(e)^{\frac{n_1}{m_1}}\right) \end{aligned} \tag{11b}$$

$$U_b = k_1 sign(s) + k_2 sign(s)^{1+\gamma_2} + k_3 sign(s)^{\frac{n_2}{m_2}} \tag{11c}$$

where $\gamma_1 = \frac{q_1}{2p_1}(1 + sgn(|e| - 1))$ under conditions m_1, n_1, p_1 and q_1 are positive odd integers, also $n_1 < m_1$, $p_1 < q_1$, $\beta_1 > 0, \eta_1 > 0$; $\gamma_2 = \frac{q_2}{2p_2}(1 + sgn(|s| - 1))$ under conditions m_2, n_2, p_2 and q_2 are positive odd integers and $n_2 < m_2$, $p_2 < q_2$ and $\delta \in R$.

Based on the error dynamical model in (10), we construct a second-order FEO as follow [4]. The observer is established to estimate the system's uncertainties as

$$\begin{aligned} \dot{z}_0 &= \upsilon_0 + \frac{1}{M}U + N_0(x) + \sigma(t) - \ddot{x}_r \\ \upsilon_0 &= -\lambda_0 K^{\frac{1}{3}} \left|z_0 - x_2\right|^{\frac{2}{3}} sign\left(z_0 - x_2\right) + z_1 \\ \dot{z}_1 &= \upsilon_1 \\ \upsilon_1 &= -\lambda_1 K^{\frac{1}{3}} \left|z_1 - \upsilon_0\right|^{\frac{1}{2}} sign\left(z_1 - \upsilon_0\right) + z_2 \\ \dot{z}_2 &= -\lambda_2 K\, sign\left(z_2 - \upsilon_1\right) \end{aligned} \ . \tag{11d}$$

where λ_0, λ_1, λ_2, and K are the positive observer gains to be designed, $z_0 = \hat{x}_2$, $z_1 = \hat{\sigma}$ and $z_2 = \hat{\dot{\sigma}}$. They are the estimations of x_2, σ and $\dot{\sigma}$ respectively.

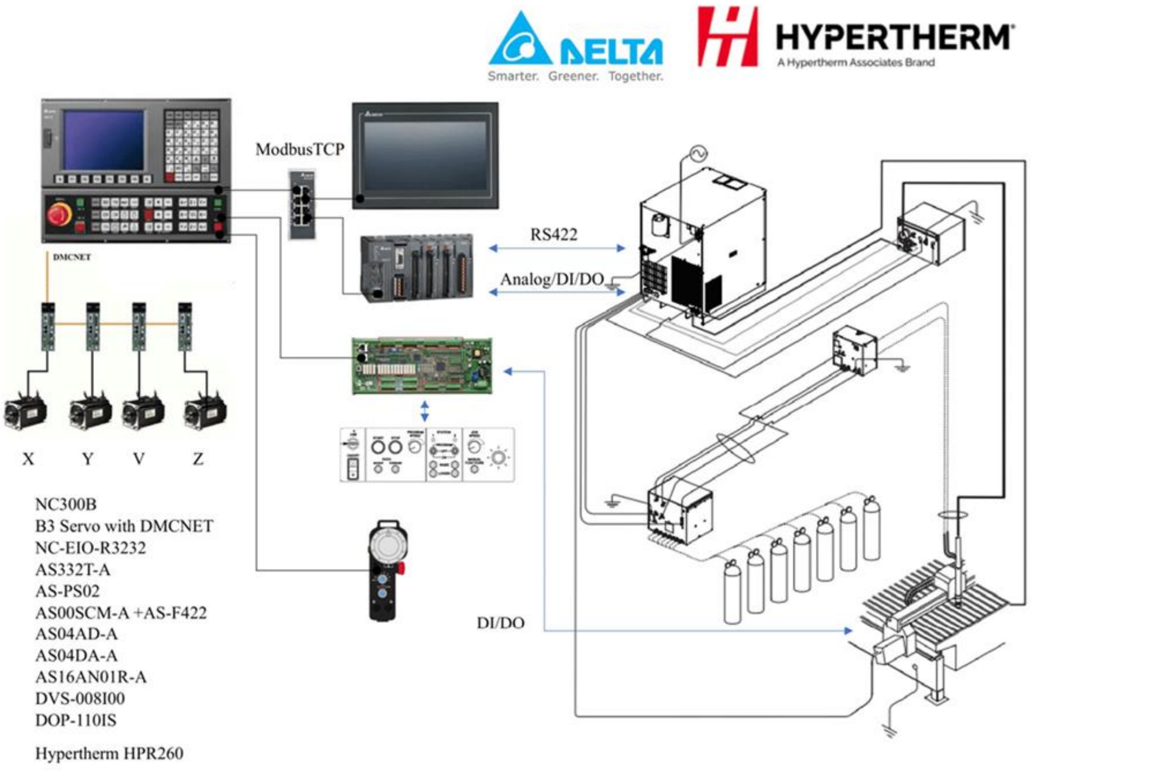

Fig. 3 Connection diagram between Delta CNC Controller and HPR260 Hypertherm Plasma Module.

Taking the observer errors as $\varepsilon_0 = z_0 - x_2$, $\varepsilon_1 = z_1 - \sigma$ and $\varepsilon_2 = z_2 - \dot{\sigma}$ we obtain the observer error equation as

$$\begin{aligned} \dot{\varepsilon}_0 &= -\lambda_0 K^{\frac{1}{3}} \left|\varepsilon_0\right|^{\frac{2}{3}} sign\left(\varepsilon_0\right) + \varepsilon_1 \\ \dot{\varepsilon}_1 &= -\lambda_1 K^{\frac{1}{3}} \left|\varepsilon_1 - \dot{\varepsilon}_0\right|^{\frac{1}{2}} sign\left(\varepsilon_1 - \dot{\varepsilon}_0\right) + \varepsilon_2 \ . \\ \dot{\varepsilon}_2 &= -\lambda_2 K \, sign\left(\varepsilon_2 - \dot{\varepsilon}_1\right) + [-K, K] \end{aligned} \tag{12}$$

It follows from the proof in [5] that all the estimated terms ε_0 and ε_1 . Their changing rates are always bounded, and in particular, ε_0 and ε_1 will converge to zero in a finite time.

Proposition 2 : By using Lemma 2, choosing the novel sliding mode surface as:

$$s = \dot{e} + \frac{1}{\Xi(e)}\left(\beta_1 sign(e)^{1+\gamma_1} + \eta_1 sign(e)^{\frac{n_1}{m_1}}\right). \tag{13}$$

Derivative (13)

$$\begin{aligned} \dot{s} &= g(x_1, x_2)u + N_0(x) + \sigma(t) - \ddot{x}_r \\ &+ \frac{1}{\Xi(e)}\left(\beta_1(1+\gamma_1)diag(|e|)^{\gamma_1} + \frac{\eta_1 n_1}{m_1} diag(e)^{\frac{n_1}{m_1}}\right) . \\ &- \frac{\dot{\Xi}(e)}{\Xi^2(e)}\left(\beta_1 sign(e)^{1+\gamma_1} + \eta_1 sign(e)^{\frac{n_1}{m_1}}\right) \end{aligned} \tag{14}$$

Substituting (11) into (14) yields:

$$\begin{aligned} \dot{s} &= \frac{1}{M}\left[M(U_{eq} + U_b - N_0(x) - \hat{\sigma})\right] + N_0(x) + \sigma(t) - \ddot{x}_r \\ &+ \frac{1}{\Xi(e)}\left(\beta_1(1+\gamma_1)diag(|e|)^{\gamma_1} + \frac{\eta_1 n_1}{m_1} diag(e)^{\frac{n_1}{m_1}}\right) \\ &- \frac{\dot{\Xi}(e)}{\Xi^2(e)}\left(\beta_1 sign(e)^{1+\gamma_1} + \eta_1 sign(e)^{\frac{n_1}{m_1}}\right) \end{aligned} \tag{15}$$

Applying (11), equation (14) is actually

$$\dot{s} = -U_b - \Gamma(t) \tag{16}$$

where $|\hat{\sigma} - \sigma(t)| \le |\Gamma(t)|$ and uncertainties tracking $|\Gamma(t)|$ is bounded by positive ξ constant. The generic close loop dynamical system illustrated in Fig. 4.

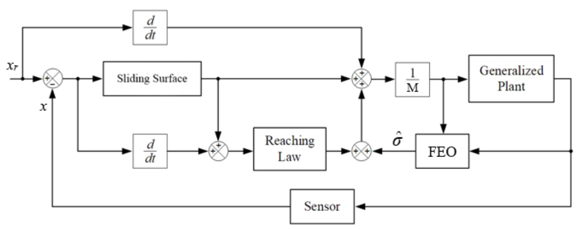

Fig. 4 The block diagram of FTSMC and FEO.

2.5 Stability Proof

The dynamical system of Plasma's Torch is a practical fixed-time stable. The controller will draw the tracking error into a set neighborhood of origin. The complete proof can be found in [7].

Proof: Chosen Lyapunov function as

$$V = \frac{1}{2}s^2. \tag{17}$$

Taking the derivative of (17) along with (15) and recalling Definition (iii), this lead to

$$\begin{aligned} \dot{V} &= s\dot{s} \\ &= s(-U_b - \Gamma(t)) \end{aligned} \tag{18}$$

Substituting (11) into (18), we have

$$\begin{aligned} \dot{V} &= -s(k_1 sign(s) + k_2 sign(s)^{1+\gamma_2} + k_3 sign(s)^{\frac{n_2}{m_2}} + \Gamma(t)) \\ &\le -k_1 s - k_2 s^{\gamma_2+2} - k_3 s^{\frac{m_2+n_2}{m_2}} + \xi s \\ &\le -k_2 s^{\gamma_2+2} - k_3 s^{\frac{m_2+n_2}{m_2}} - (k_1 - \xi)s \\ &\le -\alpha_1 V^{\frac{\gamma_2+2}{2}} - \alpha_2 V^{\frac{m_2+n_2}{2m_2}} + \nu \end{aligned} \tag{19}$$

As long as $\alpha_1, \alpha_2 > 1$ and $k_1 > \xi$, (19) is satisfied.

From Lemma 1, s reaches for the region near origin as

$$\Phi_1 = s \le \min\left\{ \left(\frac{\nu}{(1-\varsigma)\nu_1}\right)^{\frac{2}{\gamma_2+1}}, \left(\frac{\nu}{(1-\varsigma)\nu_2}\right)^{\frac{2m_2}{m_2+n_2}} \right\} \tag{20}$$

within a fixed-time given by

$$T_1 \le \frac{2}{\alpha_1\varsigma\gamma_2} + \frac{2}{\alpha_2\varsigma(m_2-n_2)} \tag{21}$$

with $\varsigma \in (0,1)$.

From Lemma 2, e is toward to the set of Φ_2, where

$$\Phi_2 = |e| \le \max\left\{ \left(\frac{\Xi\Omega'}{\beta_1}\right)^{\frac{1}{\gamma_1+1}}, \left(\frac{\Xi\Omega'}{\eta_1}\right)^{\frac{m_1}{n_1}} \right\}. \tag{22}$$

T_2 is the summation of both practical fixed time from (4) and system tracking error (9). A Fixed time response of dynamical system (16) is

$$\begin{aligned} T_2 \le \max&\left\{ \frac{n_1}{\beta_1^* m_1} + \frac{m_1}{m_1-n_1}\frac{1}{\beta_1^*}\ln\left(1+\frac{\beta_1^*}{\eta_1}\right) \right. \\ &\left. , \frac{n_1}{\beta_1 m_1} + \frac{m_1}{m_1-n_1}\frac{1}{\beta_1}\ln\left(1+\frac{\beta}{\eta_1^*}\right) \right\} \\ &+ \frac{2}{\alpha_1\varsigma\gamma_2} + \frac{2}{\alpha_2\varsigma(m_2-n_2)} \end{aligned} \tag{23}$$

where $\beta_1^* \triangleq \beta_1 - \frac{\Xi(e)S}{sign(e)^{1+\gamma_1}} > 0$ and $\eta_1^* \triangleq \eta_1 - \frac{\Xi(e)S}{sign(e)^{n_1/m_1}} > 0$.

3. Simulation Results

The simulations are provided to evaluate the proposed strategy. FTSMC is simulated with a fixed value of lump disturbances as $D = 0.2\sin(5t+0.4)$. The control parameters are set as $q_1 = q_2 = 15$, $p_1 = p_2 = 11$, $n_1 = n_2 = 13$, $m_1 = m_2 = 14$, $\beta_1 = 1$, $\eta_1 = 2$, $a_1 = 0.6$, $b_1 = 18$, $c_1 = 13$, $\gamma_1 = 12$, $\gamma_2 = 5$, $\mu_1 = 2$ and $\mu_2 = 0.04$. FEO parameters are $\lambda_0 = 5$, $\lambda_1 = 10$, $\lambda_2 = 20$ and $K = 1$. The initial condition $\omega_0 = 0$, $x_0 = 0$, $\hat{\delta}_0 = 0$. In Fig. 7 - 8, the graphic comparisons are demonstrated. FTSMC shows the better performance than the high gain PID Controller but there exits small amount of steady state error. The composite FTSMC-FEO yields better smooth response against uncertainties and no overshoot. The steady error caused by uncertainties is disappeared. The steady state response is almost identical to the reference.

4. Experimentation

The experiment began by retrofitting a CNC Plasma that had been unusable for more than 5 years. Delta CNC Control model NC300b was selected as the controller which supports G-Code programming. Four sets of servos were installed: the X-axis with a power of 750W; the Y-V axes which work in gantry mode, requiring two sets of 750W servos; and the Z-axis requiring a 400W servo with brake. Z Lifting Axis also performs Torch Height Control. In addition, to ensure that the control of the 26,000W Hypertherm Plasma Module is efficient. Delta PLC AS300 Series which supports Ladder programming, C-Like programming, 32-bits mode and high processing speed is also installed. A Delta HMI is also furnished for friendly human machine interfacing. CNC Controller, AS300 PLC and HMI exchange all data via Modbus/TCP. The connection diagram between Delta CNC Controller, HMI and HPR260 Hypertherm Plasma Module shown in Fig. 3. The samples of cutting mild steel thickness 15mm, 20mm and 25 mm with difference cutting currents are displayed in Fig.5. The retrofitted machine is shown in Fig. 6.

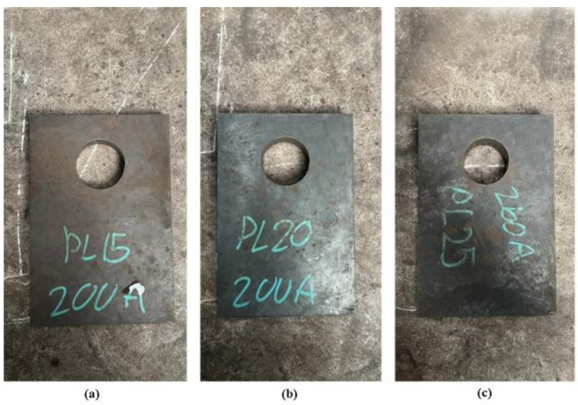

Fig. 5 Mild steel cutting samples with difference thickness: (a) 15mm-200A; (b) 20mm-200A; (c) 25mm-260A.

(a) (b) (c)

Fig. 6. (a) Plasma Machine; (b) Mild Steel Cutting Process; (c) Electrical Control Equipment.

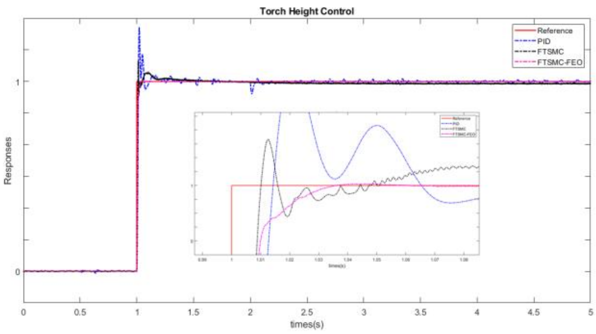

Fig. 7 Transient response.

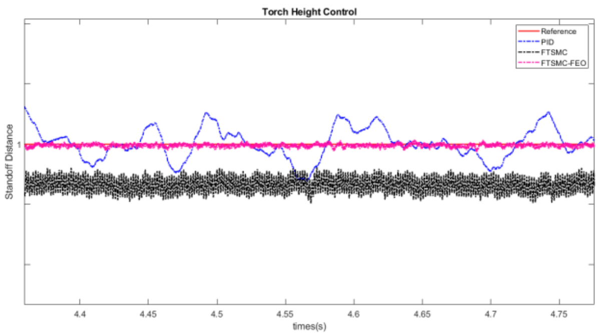

Fig. 8 Steady state response.

5. Conclusion

In this article, a further development of nonlinear controller with observer is described. A fixed-time controller is utilized for a THC to improve Plasma Arc performance , avoid singularity. To overcome the uncertainties caused by the momentum of the plasma jet , drag force, unmodelled parameters, the observer based control method is constructed to compensate the system's uncertainties. The stability is proved by well-known Lyapunov method. The reaching time towards a neighborhood of equilibrium is demonstrated. The residual sets are derived. By numerical simulations, the fixed-time controller shows better performance than PID Controller. FTSMC has a quick transient response, reduces chattering phenomenon , possesses strong robustness, singularity-free. FTSMC-FEO yields better smooth performance under system's uncertainties and external disturbances. The machine owner has spent totally about 1,000,000 baht for this project. It costs only 12.5% comparing to buying a new one. For further study, more complicated experimentation should be conducted to verify the control strategy. Deep information such as arc voltage, arc current, uncertainties estimation and compensations should be graphically exhibited.

References

[1] D. K. Naik and K. Maity, "Experimental analysis of the effect of gas flow rate and nature on plasma arc cutting of hardox-400," *Welding in the World*. 2020, vol. 64, pp. 345 – 352.

[2] J. Deli, Y. Bo and Z. Fengjing, "Decoupling Control based on PID Neural Network for Plasma Cutting System," *27th Chinese Control Conference*. 2008, pp. 659 – 662.

[3] A. Levant, "Robust exact differentiation via sliding mode techniques," *Automatica,* vol.34, no.3 , pp.379-384, Mar. 1998.

[4] Y. B. Shtessel, I. A. Shkolnikov, and A. Levant, "Smooth second-order sliding modes: Missile guidance application," Automatica, vol.43, no.8, pp. 1470-1476, Aug. 2007.

[5] V. Cholahan, T. Suwannatat, "A Robust Practical Fixed-Time Torch Height Control by Applying Arc Voltage Feedback for CNC Plasma Machines," 17th EENET 2025, pp.329-332.

[6] J. Ni, L. Liu, C. Liu, X. Hu and S. Li, " Fast fixed-time nonsingular terminal sliding mode control and its application to chaos suppression in power system," *IEEE Trans. Circuits Syst. II Express Briefs* . 2017, vol. 64, pp. 151–155.

[7] V. Cholahan, N. Wongvanich and W. Tangsrirat , "A Novel Practical Fixed-Time Speed Control of Permanent Magnet Synchronous Motors," *4th ICA-SYMP. 2025*, pp. 74-79.